Published OnlineFirst June 11, 2020; DOI: 10.1158/1078-0432.CCR-19-2570

Comparing Circulating Tumor Cell Counts with Dynamic Tumor Size Changes as Predictor of Overall Survival: A Quantitative Modeling Framework

Ida Netterberg[1], Mats O. Karlsson[1], Leon W.M.M. Terstappen[2], Miriam Koopman[3], Cornelis J.A. Punt[4], and Lena E. Friberg[1]

ABSTRACT

Purpose: Quantitative relationships between treatment-induced changes in tumor size and circulating tumor cell (CTC) counts, and their links to overall survival (OS), are lacking. We present a population modeling framework identifying and quantifying such relationships, based on longitudinal data collected in patients with metastatic colorectal cancer (mCRC) to evaluate the value of tumor size and CTC counts as predictors of OS.

Experimental Design: A pharmacometric approach (i.e., population pharmacodynamic modeling) was used to characterize the changes in tumor size and CTC count and evaluate them as predictors of OS in 451 patients with mCRC treated with chemotherapy and targeted therapy in a prospectively randomized phase III study (CAIRO2).

Results: A tumor size model of tumor quiescence and drug resistance was used to characterize the tumor size time-course, and was, in addition to the total normalized dose (i.e., of all administered drugs) in a given cycle, related to the CTC counts through a negative binomial model (CTC model). Tumor size changes did not contribute additional predictive value when the mean CTC count was a predictor of OS. Treatment reduced the typical mean count from 1.43 to 0.477 (HR = 3.94). The modeling framework was applied to explore whether dose modifications (increased and reduced) would result in a CTC count below 1/7.5 mL after 1 to 2 weeks of treatment.

Conclusions: Time-varying CTC counts can be useful for early predicting OS in patients with mCRC, and may therefore have potential for model-based treatment individualization. Although tumor size was connected to CTC, its link to OS was weaker.

Introduction

Tumor burden, most frequently evaluated as the sum of longest diameters (SLD) according to the RECIST (1, 2), may provide a foundation of evidence for treatment efficacy. However, it is desired to identify new and preferably early markers of treatment responses since changes in tumor size is delayed in relation to initiation of therapy. Circulating tumor cell (CTC) count has emerged as a possible prognostic and predictive biomarker in oncology over the past couple of decades. Measurement of the CTC count in blood is generally referred to as a liquid biopsy, which is minimally invasive and offer a simple, fast, and cost-efficient way of following disease status (3). CTCs are tumor cells that circulate in the blood after shedding from the primary tumor which may, if surviving the hostile environment in the vasculature and the transport through the narrow blood vessels, invade a distant location and metastasize a new organ (4). However, not only do CTCs have a low abundance in the blood (approximately 1 CTC per 1×10^9 blood cells in an "average" patient), but currently available assays have low sensitivity to detect all heterogeneous CTC forms. Therefore, it is common that a large proportion of samples drawn to measure the CTC count has no detectable CTC (5–9). Detectable CTC counts has however been related to worse OS and/or progression-free survival across tumor types in numerous studies (6, 7, 10–13).

The benefit of pharmacometric modeling in oncology has been frequently reported over the past couple of decades (14–19). This powerful tool may facilitate drug development in a number of aspects, including prediction of clinical outcome from preclinical data and guidance of dosing strategies, as well as optimizing treatment in the individual patient by applying personalized treatment. Although, there is still a rather limited use of these models in the clinical oncology setting, but it could be improved by closer collaborations between the treating physician and pharmacometricians, and development of user-friendly software. To our knowledge, no pharmacometric analysis has explored the relationship between changes in tumor size and CTC count and OS. Therefore, a population tumor size model was developed, on the basis of clinical data from patients with metastatic colorectal cancer (mCRC) treated with first-line chemotherapy and targeted therapy in the multicenter phase III CAIRO2 trial (20). Subsequently, a model characterizing dynamic changes in the CTC count in the same patient population was developed where the tumor size model was used to explore potential relationships between longitudinal changes in tumor size and CTC counts. Finally, variables derived from both the tumor size and CTC models were explored as predictor of OS.

Materials and Methods

Patients and data

To perform the analysis described in the sections below, data from a relatively large study with longitudinal measurements of CTC counts,

[1]Department of Pharmaceutical Biosciences, Uppsala University, Uppsala, Sweden. [2]Department of Medical Cell BioPhysics, Faculty of Science and Technology, University of Twente, Enschede, the Netherlands. [3]Department of Medical Oncology, University Medical Centre Utrecht, Utrecht University, Utrecht, the Netherlands. [4]Department of Medical Oncology, Amsterdam University Medical Centres, University of Amsterdam, Amsterdam, the Netherlands.

Note: Supplementary data for this article are available at Clinical Cancer Research Online (http://clincancerres.aacrjournals.org/).

Corresponding Author: Lena E. Friberg, Uppsala University, Box 591, Uppsala 75124, Sweden. Phone: 461-847-14685; Fax: 461-847-14003; E-mail: lena.friberg@farmbio.uu.se

Clin Cancer Res 2020;26:4892–900

doi: 10.1158/1078-0432.CCR-19-2570

Published OnlineFirst June 11, 2020; DOI: 10.1158/1078-0432.CCR-19-2570

Translational Relevance

Much attention has been directed to biomarker research in oncology, especially in the era of personalized treatment. Detailed understanding of the interplay between potential biomarkers of response and a clinical endpoint may be obtained by exploring dynamic biomarker changes following treatment initiation. Circulating tumor cell (CTC) counts have been suggested as an earlier and simpler method than tumor size scans to evaluate treatment response. Relationships between drug exposure, tumor size (sum of longest diameter), CTC count, and overall survival (OS) were quantified in patients with metastatic colorectal cancer, using a population modeling approach. The CTC time-course predicted OS. Drug treatment, and to a smaller extent, tumor size, predicted the CTC time-course. The potential value of a modified dose was explored with the aim of achieving a mean CTC count <1/7.5 mL, which indicated clinical benefit by the developed model, after 1 to 2 weeks.

tumor size, and OS were required. CTC counts were available in 458 patients treated for mCRC in the CAIRO2 trial (13, 20) and included in the current analysis. The study was conducted in agreement with the declaration of Helsinki and approved by the Committee on Research Involving Human Subjects Arnhem-Nijmegen. All patients provided written informed consent before study entry. Anticancer treatment was administered in cycles of 3 weeks. Treatment with capecitabine (1,000 mg/m^2, or 1,250 mg/m^2 after the sixth cycle as mono-chemotherapy, orally twice daily on days 1–14), oxaliplatin (130 mg/m^2 i.v. on day 1, for a maximum of six cycles) and bevacizumab (7.5 mg/kg i.v. on day 1) was administered to 230 patients (CB regimen). The same treatment schedule, with the addition of cetuximab (400 mg/m^2 i.v. on day 1 of the first cycle and 250 mg/m^2 i.v. on day 1 of the subsequent cycles) was administered to 228 patients (CBC regimen). Treatment was continued until the occurrence of disease progression, death, or unacceptable adverse event. Additional study details are available elsewhere (20). Individual dosing histories, but no drug concentrations, were available. A summary variable of all administered doses, that is, the total normalized dose (TND), was created to explore relationships between drug treatment and tumor size and CTC changes. Each administered dose was normalized to the nominal dose level and values below and above 1 therefore corresponded to a dose lower or higher than the nominal dose level, respectively. Subsequently each administered normalized dose was added to the TND. The TND was consequently 3 for a patient that received the nominal dose level for each of three different drugs.

Tumor size, that is, SLD, was measured before start of treatment and subsequently every 9 weeks using computed tomographic imaging, and evaluated with RECIST 1.0 (1). The CTC count was measured pretreatment and after 1 to 2, 3 to 5, and 6 to 12 weeks after start of treatment, and subsequently every 9 weeks, that is, at the same time as SLD evaluation, for up to a year. CTC isolation and enumeration was performed in duplicates (due to expected low CTC counts) of 7.5 mL blood each with the CellSearch System (Menarini Silicon Biosystems), which is the only system cleared by the Food and Drug administration for CTC enumeration (13, 21).

Tumor size and dropout models

A tumor size model was developed to explore the relationship between time-courses of both tumor (SLD(t)) and CTC count and OS. The primary goal of the tumor size model was therefore to characterize the individual dynamic changes well in relation to the observed tumor sizes. The tumor growth inhibition model, as suggested by Claret and colleagues (22), and the tumor size model of tumor quiescence and drug-resistance (23, 24), were explored to describe changes in SLD. In the latter model, a fraction of the total SLD is present as drug-sensitive tumor while the remaining fraction is drug-resistant. The drug-resistant tumor cells are hypothesized to transfer from an initial quiescent state to a proliferative state (**Fig. 1**), with either a fast or slow rate from the quiescent to the proliferating state ($k_{Delay,fast}$ and $k_{Delay,slow}$). Linear and exponential growth rates were evaluated. TND was explored as a predictor of SLD changes. The potential existence of different patient populations with different patterns in tumor size change (e.g., those with long and durable tumor response, tumor response followed by regrowth or tumor growth without response), together with skewed and bimodal distributions of the random effects (25), were investigated to account for the time-varying SLD measurements.

Because dropout from the study and continued measurements did not occur at random but depended on progression and the observed tumor size, a dropout model (using logistic regression) was developed to evaluate the tumor size model with simulation-based diagnostics, that is, visual predictive checks (VPC; ref. 26). Tumor size-related variables, derived from observed tumor sizes, described in **Table 1** together with time, were explored as predictors of dropout.

CTC model

The distribution of CTC counts was described by estimating the dynamic changes over time of the mean CTC count in 7.5 mL blood, that is, $\lambda_{CTC}(t)$, by applying count models of the Poisson type (i.e., Poisson, zero-inflated Poisson and negative binomial; ref. 27). $\lambda_{CTC}(t)$ does consequently not reflect an actual CTC count (integer), but is a continuous real number. Model-derived tumor size metrics, described in **Table 1**, together with the observed baseline tumor size (BTS) were explored as predictors of $\lambda_{CTC}(t)$. Effect delays were evaluated and modeled through addition of an effect compartment (28). A categorical treatment effect, that is, drug or no drug, together with drug effects based on the TND and kinetic–pharmacodynamic modeling (29) given the TND, were also tested as predictors of $\lambda_{CTC}(t)$ on top of potential tumor size-related relationships.

OS model

A parametric time-to-event model approach was used to characterize the OS data. Exponential, Weibull, Gompertz, log-normal, and log-logistic distributions were explored to describe the event times. Observed BTS, and other baseline covariates, that is, observed CTC count (BCTC), age, arm, normal/increased lactate dehydrogenase, prior chemotherapy, and resection of primary tumor, were first explored as predictors of OS in a stepwise manner, that is, the covariate that resulted in the largest improvement in the model fit (i.e., lowest P value) was included in the model in the first step and remaining covariates were subsequently re-evaluated on top of that covariate in the following step(s). Model-derived tumor size- and CTC-related metrics (described in **Table 1**) were explored, and their predictive properties were hence compared with each other (i.e., the variable resulting in the lowest P value was included in the OS model), when no additional baseline covariate improved the model fit statistically significant. The SLD(t) was extrapolated until the event time (censored or death), to a maximum of 1000 mm to avoid unrealistically large tumor sizes. Model-derived predictors were first explored one by one and then in combination, in the same way as described above for

Published OnlineFirst June 11, 2020; DOI: 10.1158/1078-0432.CCR-19-2570

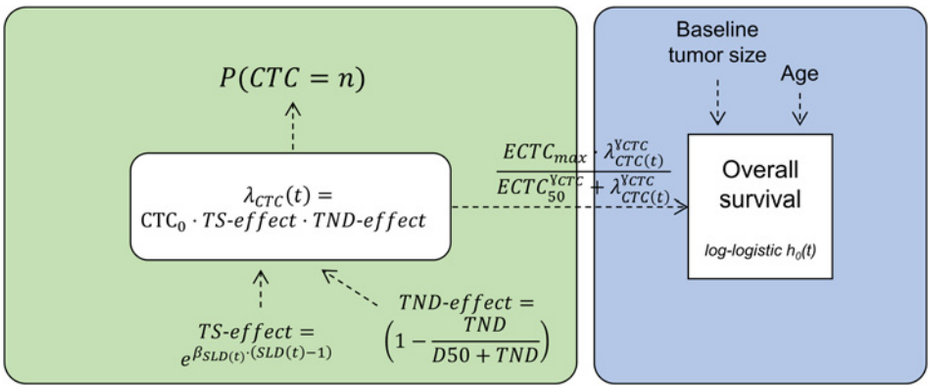

Figure 1.

Schematic representation of the final modeling framework, including the CTC (green box) and OS (blue box) models. The $\lambda_{CTC}(t)$ is affected by tumor size- and dose-related effects (TS and TND effects, respectively) and drives the probability of observing a CTC count = n. A log-logistic distribution of the baseline hazard [$h_0(t)$] for distribution of event times (death or censored) was used in the final model together with BTS, age, and $\lambda_{CTC}(t)$ (parametrized as a sigmoidal E_{max} model with the maximum effect, $ECTC_{max}$, $\lambda_{CTC}(t)$ value that gives half of $ECTC_{max}$, $ECTC_{50}$, and the steepness factor, γ_{CTC}) as predictors. Parameters in this figure that are estimated: CTC_0, $\beta_{SLD\text{-}CTC}$, D50, $ECTC_{max}$, $ECTC_{50}$, and γ_{CTC}. $\beta_{SLD\text{-}CTC}$, parameter relating SLD(t) to the mean CTC count; CTC_0, baseline mean of CTC count per mm SLD; D50, TND accounting for 50% of the maximum drug-related effect.

baseline covariates. The statistical significance of included predictors (baseline and model-derived) were finally evaluated in a backward elimination step. All predictors were added exponentially to $h_0(t)$ and additively to each other. It was also explored if a potential relationship between CTC and OS depended on if the patient had progressive disease at any time during the study period.

The performed OS analysis is consequently different compared with the analysis by Tol and colleagues, where Kaplan–Meier (KM) curves were compared using the log-ranking test and predictors of OS were evaluated using Cox proportional hazard models (13).

Data analysis

The current analysis was performed with NONMEM 7.4 (30). Parameters were estimated with the first-order conditional estimation method with interaction (tumor size model) and the Laplacian estimation method (CTC and OS models). The by NONMEM provided objective function value (OFV, i.e., −2·log likelihood) was used to guide model building, in combination with inspection of VPCs and parameter uncertainty. A significance level of $P < 0.05$ (tumor size and CTC models) or $P < 0.01$ (OS model) were used to discriminate between nested models. Additional description of the model selection and evaluation processes is presented in the Supplementary Materials and Methods.

Results

A schematic representation of the developed modeling framework (including the CTC and OS models) is presented in **Fig. 1**. All final parameter estimates and corresponding relative standard errors (RSE) are presented in **Table 2**.

Patients and data

Four hundred sixty-seven patients were eligible and enrolled between August 2005 and December 2006. The median TND across all administered doses was 3.34 (range: 0.301–23.4). The median TND in the CB and CBC groups were 2.49 (range: 0.301–23.4) and 3.93 (range: 0.370–8.52), respectively. Nine patients were excluded in the current analysis since they were lacking SLD and/or CTC measurements. Inconsistent and unexpected SLD time-courses, that is, multiple phases of increasing or decreasing SLD, were observed in 7 patients during visual inspection of the raw data. An additional 18 SLD measurements in 16 patients deviated more than clinically plausible from the other SLD observations. It was not possible to capture these dynamic changes with the explored tumor size models and these seven patients and 18 observations were therefore defined as outliers and excluded from the current analysis. There were consequently 451 patients in the analysis data set. The reasons for exclusion from the original 467 eligible patients, together with the observed SLD time-courses in the 7 patients that were excluded after visual inspection of the data, are summarized in Supplementary Fig. S1. The median SLD at baseline was 87 mm (range: 10–494 mm), the median number of SLD measurements per patient was 4 (range: 1–20) and the median follow-up time for SLD evaluation was 33 weeks (range: 0–244 weeks). The median number of CTC replicates per patient was 5 (range: 1–27) and the median follow-up time for CTC enumeration was 27 weeks (range: baseline–104 weeks). The median CTC count across all evaluable samples was 0 (range: 0–823) and there were 0 CTCs in 76% of all CTC samples. The CTC count was 0 in 51% of the baseline samples. Baseline characteristics of these 451 patients are available in Supplementary Table S1. A total of 353 of these patients died during the follow-up period and 98 were censored. The median OS was 1.7 years and follow-up ranged between 1.5 weeks and 5.1 years.

Tumor size and drop-out models

The tumor size model of tumor quiescence and drug-resistance resulted in the best model fit to the SLD data (schematically illustrated in Supplementary Fig. S2). This model did however not describe the individual dynamic changes well in patients that progressed immediately after start of treatment. None of the evaluated bimodal or skewed distributions improved the prediction of these patients, whereas addition of a third subpopulation (with a fast growth rate of the drug-sensitive fraction) resulted in better characterization of the data from these individuals. A linear growth rate of the drug-sensitive fraction described the data better than other functions of growth. No dose–response relationship could be established in the tumor size model. The individual predictions were in general in good agreement

Published OnlineFirst June 11, 2020; DOI: 10.1158/1078-0432.CCR-19-2570

Table 1. Description of explored tumor size- and CTC-related predictors.

Predictor	Derivation	Time-varying?	Explored as a predictor of:
Tumor size-related			
Progressive disease, based on observed tumor size	20% and at least 5 mm increase in tumor size	Yes	Dropout
Normalized baseline tumor size 1	$BTS - BTS_{median}$	No	Dropout, CTC, OS
Normalized baseline tumor size 2	BTS/BTS_{median}	No	CTC
Absolute tumor time-course	$SLD(t)$	Yes	Dropout, CTC, OS
Relative change from baseline SLD(t)	$\frac{SLD(t)-SLD_0}{SLD_0}$	Yes	Dropout, CTC, OS
Baseline normalized SLD(t)	$SLD(t) - SLD_0$	Yes	CTC, OS
Relative change from lowest SLD(t)	$\frac{SLD(t)-SLD_{min}}{SLD_{min}}$	Yes	CTC, OS
Time-course of rate of tumor size changes	Derivative $- SLD(t)$	Yes	CTC, OS
Categorical effect (before/after regrowth)		No	CTC
Tumor size ratio at week 9	Time <9 weeks: $SLD(t)/SLD_0$ Time ≥9 weeks: $SLD(t)_{week9}/SLD_0$	Yes (until week 9)	OS
Tumor size ratio at week 18	Time <18 weeks: $SLD(t)/SLD_0$ Time ≥18 weeks: $SLD(t)_{week18}/SLD_0$	Yes (until week 18)	OS
Time to tumor growth, TTG	Time <TTG: Time Time ≥TTG: TTG	Yes (until time of regrowth)	OS
CTC-related			
Absolute mean CTC count, $\lambda_{CTC}(t)$		Yes	OS
Relative change from baseline $\lambda_{CTC}(t)$	$\frac{\lambda(t)-CTC_{actual,0}}{CTC_{actual,0}}$	Yes	OS
$\lambda_{CTC}(t)$ at weeks 1, 3, and 6 ($\lambda_{CTC,1w}$, $\lambda_{CTC,3w}$ and $\lambda_{CTC,6w}$)	Time <1/3/6 weeks: $\lambda(t)$ Time ≥1/3/6 weeks: $\lambda(t)_{week1/2/3}$	Yes (until week 1/3/6)	OS
$\lambda_{CTC}(t)$ ratio at weeks 1, 3, and 6	Time <1/3/6 weeks: $\lambda(t)/\lambda_{actual,0}$ Time ≥1/3/6 weeks: $\lambda(t)_{week1/2/3}/\lambda_{actual,0}$	Yes (until week 1/3/6)	OS
Categorical effect for $\lambda_{CTC}(t)$ ≥1/2/3/estimated		Yes	OS

Abbreviations: BTS, baseline tumor size; SLD_0, estimated baseline SLD; SLD_{min}, lowest SLD; $CTC_{actual,0}$, estimated baseline mean CTC count given a patient's baseline tumor size.

with the observed data. Individual SLD model-predictions in relation to their observed SLD are presented for 9 patients in Supplementary Fig. S3.

The probability of dropping out increased when the patient had progressive disease [$\theta_{PRD} = 2.05$; 95% confidence interval (CI), 1.61–2.50]. No other predictor of dropout was identified on top of progressive disease. The results (ΔOFVs and P values) for all explored dropout predictors are given in Supplementary Table S2. The VPC of the final tumor size model in Supplementary Fig. S4, taking dropout into account, demonstrates a good agreement between the observed and simulated data.

CTC model

The negative binomial model, accounting for overdispersion of the data (i.e., the mean of the data is smaller than the variance of the data), resulted in the best fit of the evaluated base CTC models. The proportion of CTC count = 0 over time was however not well characterized in the base model, as illustrated in the left panel in **Fig. 2**. An exponential function of the model-derived absolute SLD(t) improved the model fit most among the tumor size-related predictors and was therefore related to $\lambda_{CTC}(t)$ (Eq. A). No delay of the tumor size effect on $\lambda_{CTC}(t)$ could be identified. The TND was related to $\lambda_{CTC}(t)$ as described in Eq. A;

$$\lambda_{CTC}(t) = CTC_0 \cdot e^{\beta_{SLD(t)} \cdot (SLD(t)-1)} \cdot \left(1 - \frac{TND}{D50 + TND}\right) \quad (A)$$

CTC_0 is the baseline CTC count for an SLD of 1 mm and in absence of drug. $\beta_{SLD(t)}$ is a parameter relating SLD(t) to $\lambda_{CTC}(t)$ and D50 is the TND accounting for 50% of the maximum drug-related effect. $\lambda_{CTC}(t)$ and the parameter describing overdispersion (O) described the probability of observing a CTC count equal to n, according to Eq. B;

$$P(CTC = n) = \frac{\Gamma\left(n + \frac{1}{O}\right)}{\Gamma\left(\frac{1}{O} \cdot n!\right)} \cdot \left(\frac{1}{1 + O \cdot \lambda_{CTC}(t)}\right)^{\frac{1}{O}} \cdot \left(\frac{\lambda_{CTC}(t)}{\frac{1}{O} + \lambda_{CTC}(t)}\right)^{n} \quad (B)$$

where Γ and $n!$ represent the gamma function and factorial function of n, respectively.

Inclusion of SLD(t) as a predictor of $\lambda_{CTC}(t)$ improved the description of the proportion of CTC count = 0 from approximately 30 weeks after start of treatment and onwards (middle panel in **Fig. 2**), while when also adding the dose–response relationship, there was a better description of the initial increase in proportion of CTC count = 0

Published OnlineFirst June 11, 2020; DOI: 10.1158/1078-0432.CCR-19-2570

Table 2. Parameter estimates and their corresponding uncertainty (RSE) in the final tumor size, CTC (Eq. A), and OS (Eq. C) models.

Parameter	Estimate (RSE%)	IIV %CV (RSE%)
TS model		
SLD_0 (mm)	88.3 (4.2)	[a]0.586 (7.6)
Box-cox shape (IIV-SLD_0)	−0.246 (23)	
FR_{logit}	0.279 (25)	[a]2.30 (12.7)
FR (%)	56.9	
$R_{Grow,sensitive,slow}$ (mm/week)	8.38×10^{-5} (11)	
$R_{Grow,sensitive,fast}$ (mm/week)	5.02 (28)	
k_{Kill} ($week^{-1}$)	9.55×10^{-3} (7.0)	71.4 (7.9)
$k_{Delay,slow}$ ($week^{-1}$)	4.53×10^{-3} (0.41)	
$k_{Delay,fast}$ ($week^{-1}$)	66.6×10^{-3} (0.70)	57.3 (3.0)
$k_{Grow,resistant}$ ($week^{-1}$)	55.3×10^{-3} (0.32)	83.2 (7.4)
$\theta 1_{Mix,logit}$	−0.103 (230)	
$\theta 2_{Mix,logit}$	−2.37 (16)	
P(Mix 1) %	52.6[b] (41–64)	
P(Mix 2) %	39.7[b] (26–53)	
P(Mix 3) %	7.7[b] (2.4–22)	
$Error_{proportional}$	0.0889 (3.7)	17.1 (11)
$Error_{additive}$ (mm)	1.97 (1.45)	
CTC model		
CTC_0	0.704 (11)	274 (4.3)
O	1.40 (15)	732 (9.1)
$\beta_{SLD(t)}$ (mm^{-1})	8.11×10^{-3} (11)	
D50	0.503 (11)	176 (11)
OS model		
β_0	15.1 (1.2)	
γ	0.751 (4.0)	
β_{BTS} (mm^{-1})	1.37×10^{-3} (37)	
β_{Age} ($years^{-1}$)	1.41×10^{-2} (26)	
$ECTC_{max}$	7.59 (4.6)	
$ECTC_{50}$ (mean CTC count)	0.315 (2.8)	
γ_{CTC}	4.91 (3.8)	

Abbreviations: CV, coefficient of variation; SLD_0, baseline SLD; FR_{logit}, fraction drug-resistant tumor of SLD_0 estimated on logit scale; FR, corresponding actual fraction of FR_{logit}; $R_{Grow,sensitive,slow}$, slow growth rate constant of drug-sensitive fraction; $R_{Grow,sensitive,fast}$, fast growth rate constant of drug-sensitive fraction; k_{Kill}, tumor kill rate constant; $k_{Delay,slow}$, slow transit compartment delay rate constant from quiescent to tumor to drug-resistant tumor; $k_{Delay,fast}$, fast transit compartment delay rate constant from quiescent tumor to drug-resistant tumor; $k_{Grow,resistant}$, growth rate constant of drug-resistant fraction; $\theta 1_{Mix,logit}$, mixture parameter 1 estimated on logit scale; $\theta 2_{Mix,logit}$, mixture parameter 2 estimated on logit scale; P(Mix 1), proportion of patients in mixture 1 (i.e., $k_{Delay,slow} + R_{grow,sensitive,slow}$); P(Mix 2), proportion of patients in mixture 2 (i.e., $k_{Delay,fast} + R_{grow,sensitive,slow}$); P(Mix 3), proportion of patients in mixture 3 (i.e., $k_{Delay,slow} + R_{grow,sensitive,fast}$); CTC_0, baseline mean of CTC count per mm SLD in 7.5 mL blood; O, overdispersion parameter; $\beta_{SLD\text{-}CTC}$, parameter relating SLD(t) to the mean CTC count; D50, TND accounting for 50% of the maximum drug-related effect; β_0, scale parameter in the log-logistic distribution; γ, shape parameter in the log-logistic distribution; β_{BTS}, parameter relating the baseline tumor size to the hazard; β_{Age}, parameter relating age to the hazard; $ECTC_{max}$, maximum CTC effect; $ECTC_{50}$, mean CTC count that gives half of $ECTC_{max}$; γ_{CTC}, steepness factor in the sigmoidal CTC E_{max} model.

[a]IIV is reported as a variance.

[b]Corresponding 95% CI, given the uncertainty in $\theta 1_{Mix,logit}$ and $\theta 2_{Mix,logit}$.

(right panel in **Fig. 2**). A VPC showing nine different proportions of CTC counts (i.e., equal to 0, 1, 2, 3, >3 and ≤5, >5 and ≤10, >10 and ≤50, >500, and ≤100 and >100) over time revealed in general a good agreement between the observed and simulated proportions (Supplementary Fig. S5), given the final CTC model as described in Eqs. (A) and (B), in all nine categories.

OS model

The log-logistic distribution, parameterized with scale (β_0) and shape (γ) parameters, described the event times the best. γ was estimated to a value below 1, meaning that the hazard, that is, $h(t)$, is first increasing with time, t, and then decreasing monotonically. BTS, BCTC, and age were added as predictors after exploration of baseline covariates. Most of the model-derived metrics resulted in statistically significant improvement of the model fit. The most pronounced improvement was observed when $\lambda_{CTC}(t)$ through a sigmoidal E_{max} model was used to predict OS ($\Delta OFV = 149$, $P = 4.33 \times 10^{-32}$). Compared with the best tumor size-related variable, that is, absolute SLD(t), the drop in OFV was lower ($\Delta OFV = 66.6$, $P = 3.33 \times 10^{-16}$). No additional model-derived variable (including dynamic tumor size changes) improved the model fit further ($P > 0.01$). The tumor size time-course was however indirectly related to OS since the tumor size, in combination with TND, a predictor of $\lambda_{CTC}(t)$ as described above. BCTC was removed from the OS model after the backward elimination step and BTS, age, and the effect based on $\lambda_{CTC}(t)$ (CTC_{effect}) were therefore included in the final OS model, which is described in Eq. (C);

$$h(t) = \frac{(e^{-\beta_0})^{\frac{1}{\gamma}} \cdot t^{\frac{1}{\gamma}-1}}{\gamma \cdot \left(1 + (e^{-\beta_0} \cdot t)^{\frac{1}{\gamma}}\right)} \cdot e^{\left(\beta_{BTS} \cdot (BTS-87) + \beta_{Age} \cdot (Age-63) + CTC_{effect}\right)} \quad (C)$$

where β_{BTS} and β_{Age} are parameters relating the effect of BTS and age to the hazard, respectively, and the CTC_{effect} is defined as in Eq. (D);

$$CTC_{effect} = \frac{ECTC_{max} \cdot \lambda_{CTC(t)}^{\gamma_{CTC}}}{ECTC_{50}^{\gamma_{CTC}} + \lambda_{CTC(t)}^{\gamma_{CTC}}} \quad (D)$$

where $ECTC_{max}$ is the maximum effect, $ECTC_{50}$ is the $\lambda_{CTC}(t)$ value that gives half of $ECTC_{max}$ and γ_{CTC} is the steepness factor.

No relationship between progressive disease and CTC_{effect} could be identified, that is, CTC_{effect} was the same in patients with and without progressive disease.

The KM VPC of the final OS model illustrated an acceptable agreement between the observed KM curve and the 95% CI based on simulations from the final OS model (**Fig. 3**), with a slight overprediction of the survival from approximately 1 year. The continuous relationships between the relative hazard and the range of the observed BTS and age are illustrated in **Fig. 4**. The relative hazard was 1.39 (95% CI, 1.07–1.80) and 1.23 (95% CI, 1.03–1.47) for a patient with a BTS of 325 mm (i.e., the 97.5th percentile) or a 78-year-old patient, in relation to the typical patient with the median BTS (i.e., 87 mm) and age (63 years) and $\lambda_{CTC}(t) < 1$, respectively, given the final parameter estimates of β_{BTS} and β_{Age} (presented in **Table 2**). Including BTS and age as predictors of OS resulted in an improved description of the mean change of these variables in the population over time (Supplementary Fig. S6). The sigmoidal E_{max} model predicted a steep relationship between $\lambda_{CTC}(t)$ and the prediction of OS ($\gamma = 4.91$) where the maximum effect was almost reached already for a $\lambda_{CTC}(t) = 1/7.5$ mL [i.e., 99.7% of $ECTC_{max}$]. Treatment reduced the typical $\lambda_{CTC}(t)$ from 1.43 to 0.477, resulting in a relative hazard of 3.94.

Impact of dose escalation and reduction

The CTC count was ≥1/7.5 mL in at least one replicate before start of treatment in 248 patients. The CTC model predicted a majority of the patients to have a CTC count <1/7.5 mL at 1 to 2 weeks after start of treatment, whereas 46 of the 248 patients still had a CTC count ≥1. Because the hazard of dying was higher in patients with a CTC count

Published OnlineFirst June 11, 2020; DOI: 10.1158/1078-0432.CCR-19-2570

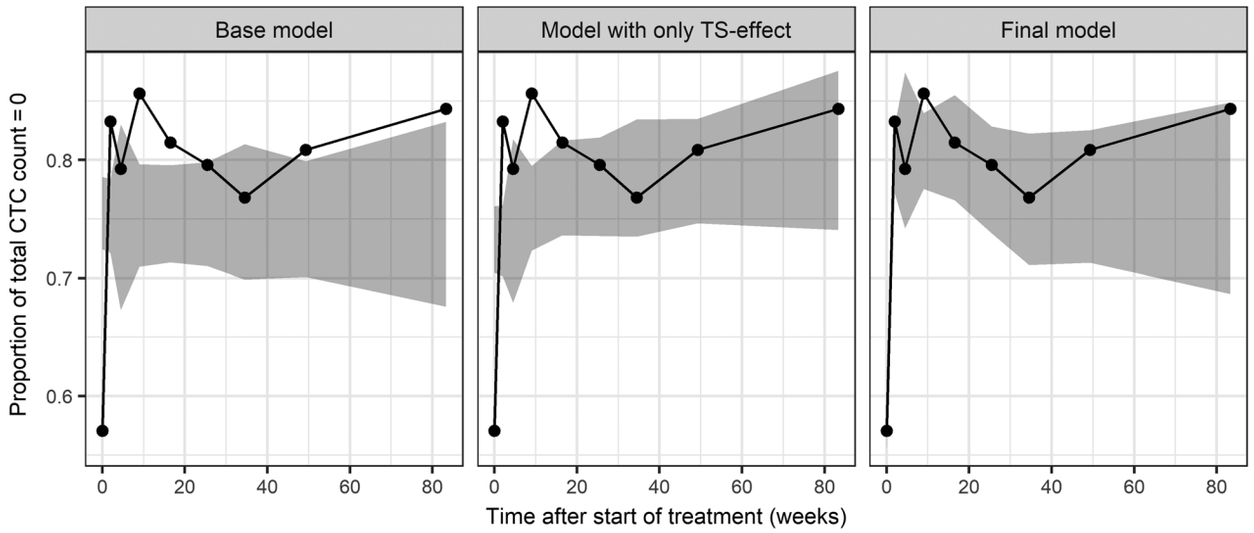

Figure 2.
VPC of the proportions of CTC count = 0 over time in the base CTC model (left), in the model including only a tumor size-related effect (middle) and the final CTC model (including both tumor size- and drug-related effects, right). The dots represent the observed proportions (connected with a line), and the shaded areas are the 95% CI of the simulated data, derived from 200 simulations from the corresponding CTC models.

≥1/7.5 mL, it was investigated if an increase in TND could result in a CTC count <1/7.5 mL at the first measurement after start of treatment in these patients, because the developed modeling framework suggested clinical value for a CTC count <1/7.5 mL. A 50% higher TND (range 3.15–8.31), a doubled TND (range 4.20–11.1) and a tripled TND (range 6.30–16.6) reduced the CTC count to below 1/7.5 mL at the first measurement after start of treatment in 7 of the 46 patients (15%) when TND was 50% higher and in 16 (35%) and 26 (57%) patients when the TND was doubled and tripled, respectively. It was also explored if a reduced TND would be acceptable with respect to retaining the CTC count <1/7.5 mL in patients with a CTC count <1/7.5 mL at the first measurement after start of treatment ($n = 148$).

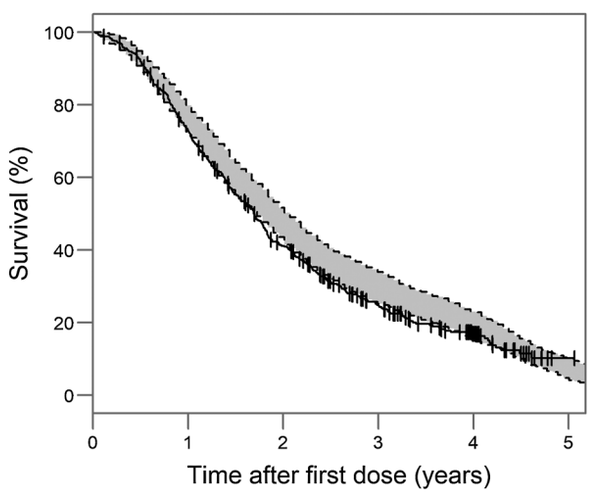

Figure 3.
KM VPC of the final OS model. The figure illustrates the observed KM curve (black line) in comparison to the 95% CI, generated from 100 simulations (gray-shaded area). Black vertical lines indicate censored events.

The model predicted the CTC count to stay below 1/7.5 mL in most of the patients, following a 25% ($n = 139$) and 50% ($n = 125$) dose reduction.

Discussion

To our knowledge, this is the first time the relationship between changes in tumor size, CTC counts over time, and OS have been quantified using a pharmacometric approach. Here we present a modeling framework that identified and established such quantitative relationships in patients with mCRC treated with first-line chemotherapy (capecitabine and oxaliplatin) and targeted agents (bevacizumab and cetuximab) in the CAIRO2 trial (20). Parts of the data included in the current nonlinear mixed effects analysis and parametric time-to-event analysis have been analyzed previously, using Cox proportional hazards models, where the CTC count was also found to be related to OS (13). However, the current analysis added mechanistic and quantitative understanding of the relationship between dynamic changes in SLD and CTC count, as well as how these time-varying variables are related to OS. The CTC time-course, for which TND and the model-predicted SLD were covariates (Eq. A), was a better predictor of OS than the SLD time-course alone. When the model-predicted CTC time-course was included in the OS model, SLD did not improve the fit further ($P > 0.01$). In addition, a dose–response relationship was identified which could be applied for dose individualizations.

The developed tumor size model, using a similar model structure as suggested by Bender and colleagues (23, 24), was used to drive the probability of observing a CTC count of a number n, by applying a count model approach with overdispersion, that is, SLD was included as a predictor of $\lambda_{CTC}(t)$. A dose–response relationship, separate from the time-course of tumor size, was also identified as a significant driver of the CTC time-course. The TND in a given cycle inhibited the mean CTC count which captured the rapid increase in proportion of CTC counts = 0 after treatment initiation. It should however be noted that the drug

Published OnlineFirst June 11, 2020; DOI: 10.1158/1078-0432.CCR-19-2570

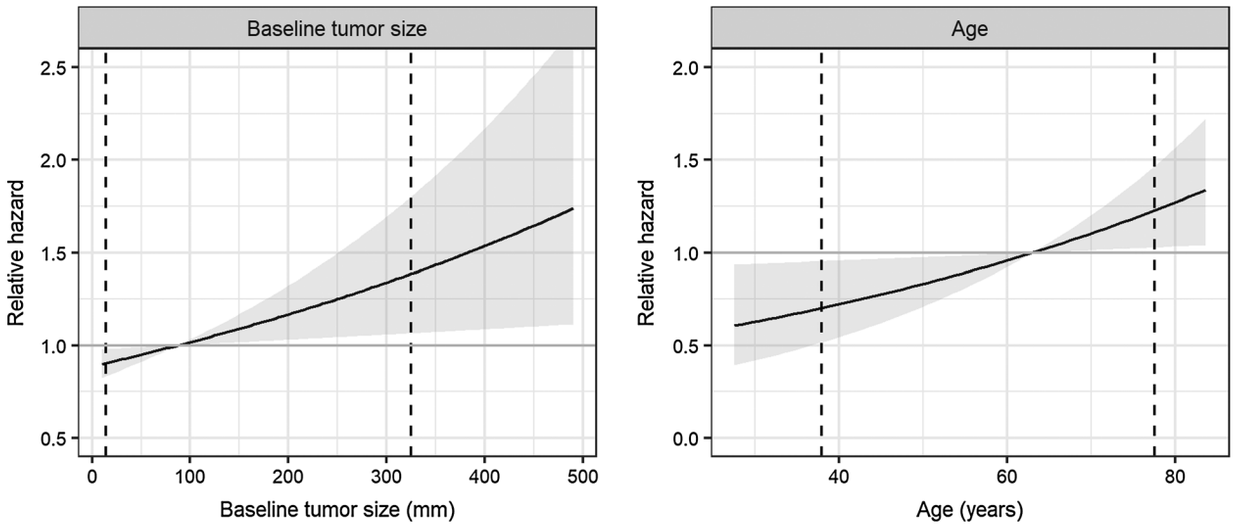

Figure 4.

Relative (to the median patient, i.e., a 63-year-old patient with a BTS of 87 mm and a $\lambda_{CTC}(t)$ <3/7.5 mL) hazard illustrated for a change in BTS (left) and age (right) given parameter estimates in the final OS model (solid black lines). Shaded areas represent the 95% CI, given the corresponding standard error. The relationships are illustrated for the observed range of the covariate value, and dashed vertical lines represent the 2.5th and 97.5th percentiles of the observed covariate value. The horizontal gray line indicates no change in relative hazard.

effect was not separated within or between the different therapies, that is, they were equally weighted. The final CTC model described the observed data well, including the large proportion (i.e., 76% of all samples) of undetectable CTCs. However, it differed in several aspects in comparison to a previously developed CTC count model (8). Wilbaux and colleagues used a lifespan model to describe the CTC kinetics and related a latent variable (to represent an underlying tumor burden) to changes in CTC counts and prostate-specific antigen (PSA; ref. 8). No direct link between PSA and CTC could however be identified. Because the addition of an effect compartment did not improve the model fit statistically significant, no further attempts were implemented to explore the lifespan model in the current analysis. Also, the latent variable in the Wilbaux model was related to virtual drug amounts in hypothetical drug compartments whereas no improvement was observed when a kinetic–pharmacodynamic model was explored in our model. Furthermore, the Wilbaux analysis did not include an analysis of OS. Although, by simulating the kinetics of PSA, CTC, and the latent variable, Wilbaux and colleagues demonstrated that the CTC count was more sensitive to changes in the latent variable compared with PSA and concluded CTC to be an earlier biomarker than PSA. Even though the models diverge on several aspects, the Wilbaux model and the CTC model presented here are similar in the sense that both use a negative binomial model to describe the dynamic changes in CTC counts. The overdispersion parameter was above 1 in both the Wilbaux model (4.9) and the current analysis (1.40), indicating that the difference between the mean CTC count and the variability in the CTC count is large. The current analysis is consequently not only the first to quantify the relationship between the longitudinal CTC time-course and OS but also to explore the predictive value of changes in tumor size and CTC count, in relation to each other, with respect to OS in a population model.

It was found that all explored tumor size-related variables in the current analysis improved the OS model fit statistically significant in the univariable analysis (i.e., with baseline covariates included only). These findings are supported by previous reports of time-varying tumor size-related model-derived variables associated to OS across both tumor and treatment types (18, 22, 31–35). However, the mean CTC time-course was the best model-derived predictor of OS and no tumor size-related variable contributed to the model fit on top of the CTC-related predictor ($P > 0.01$). It should however be noted that since SLD was related to CTC it could be regarded as an indirect predictor of OS. Both the mean CTC count and dichotomized time-courses (i.e., time-varying variables) were explored as predictors in the current analysis. The mean CTC count, parameterized as a sigmoidal E_{max} model demonstrated best model improvement. This model suggested that already for a mean CTC count of 1/7.5 mL the maximum CTC-induced increase in the hazard was reached. This threshold is however lower than what has been found previously in patients with mCRC (13, 36–38). Several studies have demonstrated evidence for the CTC count as a predictive and prognostic biomarker in oncology. The CTC count has commonly been dichotomized as above or below a threshold in such studies. Worse survival has been observed in patients with a CTC count at or above a threshold (both at baseline and as a change at a specific time after start of treatment) in patient populations including breast (≥5 CTCs/7.5 mL; ref. 39), prostate (≥5 CTCs/7.5 mL; ref. 40), colorectal (≥3 CTCs/7.5 mL; refs. 13, 36–38), and non–small cell lung cancer (≥50 CTCs/7.5 mL; ref. 41). Being the third most common cancer type as of 2018 with 1.8 million estimated new cases and 862 000 estimated deaths (42), there is an unmet need for clinically valuable biomarkers of treatment efficacy in colorectal cancer (43). However, the results in this analysis support the evidence for the CTC count as a predictive biomarker in mCRC. The use of CTC count as a biomarker to evaluate treatment response is beneficial in comparison to SLD, partly because a response is often observed earlier in the CTC count but also because CTCs reflect the total tumor burden (including target, nontarget, and new lesions) whereas SLD only represents the size (and not morphological changes which has been related to pathologic response and OS in mCRC; ref. 44) of target lesions. However, the

clinical utility to guide clinical decision making and evaluate response to treatment has been questioned (45, 46).

Liquid biopsies enable not only measurements of CTCs but also other analytes such as circulating tumor DNA (ctDNA), which is a type of circulating cell-free DNA that may reflect the tumor genome (3, 47). It has been suggested that both CTCs and ctDNA can be used to facilitate treatment decisions and that the information they provide complement each other (48). As mentioned previously, the CTC count correlates with survival, whereas ctDNA serves as a biomarker of early detection of relapse (3, 49). Exploration of relationships between dynamic changes in tumor size, CTC count, and ctDNA therefore serves as a potential extension to the here proposed modeling framework. Also, because CTC counts are commonly detected in a low number, especially in mCRC, novel biomarkers, that can be measured at a higher frequency than CTCs while also correlating with CTC counts, are being studied as a potential alternative/addition to CTC, for example, tumor-derived extracellular vesicles (tdEV). tdEVs are tumor microparticles and CTC fragments that correlate with poor prognosis across tumor types, including mCRC (50). Therefore, it would be interesting to also include tdEVs in the proposed modeling framework and explore potential relationships between tdEV and tumor size and OS, in comparison to CTC count.

Because the current modeling framework indicated that a CTC count below 1/7.5 mL, compared with ≥1/7.5 mL, is related to a better OS, it is of interest to explore if individual dose-adjustment (of the TND) would be beneficial in reducing tumor size and lead to a subsequent sufficient reduction in CTC count. Therefore, the potential utility of the developed modeling framework was explored by evaluating how increased and reduced TNDs affected the $\lambda_{CTC}(t)$ at the first measurement after start of treatment (i.e., 1–2 weeks). The CTC model predicted that 15%, 35%, and 57% of patients with a $\lambda_{CTC}(t)$ ≥1/7.5 mL at baseline and first measurement after start of treatment could achieve CTC count <1/7.5 mL at the first measurement after start of treatment with a 50% higher, doubled and tripled TND, respectively. Clinically, the risk of severe toxicity should of course be considered prior to any dose-escalation. Therefore, the impact of a reduced TND was also explored. The model predicted the CTC count to be retained below 1/7.5 mL in a majority of the patients when the TND was reduced by 25% and 50%.

The current modeling framework added mechanistic and quantitative understanding of relationships between the dynamic changes in tumor size and CTC counts and OS in patients with mCRC treated with first-line chemotherapy and targeted therapy. A positive relationship was established between the tumor size and CTC time-courses, as well as a dose–response relationship. Furthermore, the model-derived mean CTC ≥1/7.5 mL was related to worse survival, suggesting that the CTC count during treatment may be used as an indicator of treatment efficacy. However, further studies are warranted to evaluate the applicability of the models with other anticancer agents and in other cancer types.

Disclosure of Potential Conflicts of Interest

I. Netterberg reports grants from the Swedish Cancer Society. L.W.M.M. Terstappen is listed as an inventor on U.S. patents (nos.: 5,985,153, 5,993,665, 6,013,188, 6,136,182, 6,361,749, 6,365,362, 6,551,843 B1, 6,623,982 B1, 6,620,627 B1, 6,623,983 B1, 6,645,731 B2, 6,660,159 B1, 6,790,366 B2, 6,890,426 B2, 7,056,657 B2, 7,332,288 B2, 7,863,012 B2, 8,329,422 B2) related to the CellSearch system, the rights of which are assigned to Menarini. M. Koopman reports grants from Amgen, Sanofi-Aventis, Sirtex, Servier [all institutional (grant and honoraria)], Roche, Merck-Serono, Bayer, and Bristol-Myers Squibb; reports other remuneration from Servier [all institutional (grant and honoraria)], other remuneration from Nordic Farma (honoraria institutional fees), and other remuneration from Bristol-Myers Squibb (grant and honoraria institutional fees) outside of submitted work. C.J.A. Punt reports other remuneration from Bayer, Servier, and Nordic Pharma (advisory role). L.E. Friberg reports grants from Swedish Cancer Society during the conduct of this study; and grants from Genentech and other from Merck Serono (commissioned work) outside of this study. No potential conflicts of interest were disclosed by the other authors.

Authors' Contributions

I. Netterberg: Conceptualization, formal analysis, validation, investigation, visualization, methodology, writing-original draft, project administration, writing-review and editing. **M.O. Karlsson:** Supervision, investigation, methodology, writing-review and editing. **L.W.M.M. Terstappen:** Data curation, investigation, writing-review and editing. **M. Koopman:** Data curation, investigation, writing-review and editing. **C.J.A. Punt:** Data curation, investigation, writing-review and editing. **L.E. Friberg:** Conceptualization, resources, formal analysis, supervision, funding acquisition, validation, investigation, methodology, project administration, writing-review and editing.

Acknowledgments

The authors acknowledge all patients and investigators who contributed to the CAIRO2 study. The analysis was funded by the Swedish Cancer Society (CAN 2017/626).

The costs of publication of this article were defrayed in part by the payment of page charges. This article must therefore be hereby marked *advertisement* in accordance with 18 U.S.C. Section 1734 solely to indicate this fact.

Received August 8, 2019; revised January 4, 2020; accepted June 4, 2020; published first June 11, 2020.

References

1. Therasse P, Arbuck SG, Eisenhauer EA, Wanders J, Kaplan RS, Rubinstein L, et al. New guidelines to evaluate the response to treatment in solid tumors. European Organization for Research and Treatment of Cancer, National Cancer Institute of the United States, National Cancer Institute of Canada. J Natl Cancer Inst 2000;92:205–16.
2. Litière S, Isaac G, De Vries EGE, Bogaerts J, Chen A, Dancey J, et al. RECIST 1.1 for response evaluation apply not only to chemotherapy-treated patients but also to targeted cancer agents: a pooled database analysis. J Clin Oncol 2019;37:1102–10.
3. Neumann MHD, Bender S, Krahn T, Schlange T. ctDNA and CTCs in liquid biopsy - current status and where we need to progress. Comput Struct Biotechnol J 2018;16:190–5.
4. Chaffer CL, Weinberg RA. A perspective on cancer cell metastasis. Science 2011; 331:1559–64.
5. Chen L, Bode AM, Dong Z. Circulating tumor cells: moving biological insights into detection. Theranostics 2017;7:2606–19.
6. Rack B, Schindlbeck C, Jückstock J, Andergassen U, Hepp P, Zwingers T, et al. Circulating tumor cells predict survival in early average-to-high risk breast cancer patients. J Natl Cancer Inst 2014;106. pii: dju066.
7. Martín M, Custodio S, de Las Casas M-LM, García-Sáenz J-Á, de la Torre J-C, Bellón-Cano J-M, et al. Circulating tumor cells following first chemotherapy cycle: an early and strong predictor of outcome in patients with metastatic breast cancer. Oncologist 2013;18:917–23.
8. Wilbaux M, Tod M, De Bono J, Lorente D, Mateo J, Freyer G, et al. A joint model for the kinetics of CTC count and PSA concentration during treatment in metastatic castration-resistant prostate cancer. CPT Pharmacomet Syst Pharmacol 2015;4:277–85.
9. Rothé F, Maetens M, Rouas G, Paesmans M, Van den Eynde M, Van Laethem J-L, et al. CTCs as a prognostic and predictive biomarker for stage II/III colon cancer: a companion study to the PePiTA trial. BMC Cancer 2019;19:304.

10. De Laere B, Oeyen S, Van Oyen P, Ghysel C, Ampe J, Ost P, et al. Circulating tumor cells and survival in abiraterone- and enzalutamide-treated patients with castration-resistant prostate cancer. Prostate 2018;78:435–45.
11. Giuliano M, Giordano A, Jackson S, Hess KR, De Giorgi U, Mego M, et al. Circulating tumor cells as prognostic and predictive markers in metastatic breast cancer patients receiving first-line systemic treatment. Breast Cancer Res 2011; 13:R67.
12. Danila DC, Heller G, Gignac GA, Gonzalez-Espinoza R, Anand A, Tanaka E, et al. Circulating tumor cell number and prognosis in progressive castration-resistant prostate cancer. Clin Cancer Res 2007;13:7053–8.
13. Tol J, Koopman M, Miller MC, Tibbe A, Cats A, Creemers GJM, et al. Circulating tumour cells early predict progression-free and overall survival in advanced colorectal cancer patients treated with chemotherapy and targeted agents. Ann Oncol 2010;21:1006–12.
14. EFPIA MID3 Workgroup, Marshall SF, Burghaus R, Cosson V, Cheung SYA, Chenel M, et al. Good practices in model-informed drug discovery and development: practice, application, and documentation. CPT Pharmacomet Syst Pharmacol 2016;5:93–122.
15. Buil-Bruna N, López-Picazo J-M, Martín-Algarra S, Trocóniz IF. Bringing model-based prediction to oncology clinical practice: a review of pharmacometrics principles and applications. Oncologist 2016;21:220–32.
16. Mould DR, Walz A-C, Lave T, Gibbs JP, Frame B. Developing exposure/response models for anticancer drug treatment: special considerations. CPT Pharmacomet Syst Pharmacol 2015;4:e00016.
17. Venkatakrishnan K, Friberg LE, Ouellet D, Mettetal JT, Stein A, Trocóniz IF, et al. Optimizing oncology therapeutics through quantitative translational and clinical pharmacology: challenges and opportunities. Clin Pharmacol Ther 2015;97:37–54.
18. Bender BC, Schindler E, Friberg LE. Population pharmacokinetic-pharmacodynamic modelling in oncology: a tool for predicting clinical response. Br J Clin Pharmacol 2015;79:56–71.
19. Keizer RJ, Ter Heine R, Frymoyer A, Lesko LJ, Mangat R, Goswami S. Model-informed precision dosing at the bedside: scientific challenges and opportunities. CPT Pharmacomet Syst Pharmacol 2018;7:785–7.
20. Tol J, Koopman M, Cats A, Rodenburg CJ, Creemers GJM, Schrama JG, et al. Chemotherapy, bevacizumab, and cetuximab in metastatic colorectal cancer. N Engl J Med 2009;360:563–72.
21. Allard WJ, Matera J, Miller MC, Repollet M, Connelly MC, Rao C, et al. Tumor cells circulate in the peripheral blood of all major carcinomas but not in healthy subjects or patients with nonmalignant diseases. Clin Cancer Res 2004;10: 6897–904.
22. Claret L, Girard P, Hoff PM, Van Cutsem E, Zuideveld KP, Jorga K, et al. Model-based prediction of phase III overall survival in colorectal cancer on the basis of phase II tumor dynamics. J Clin Oncol 2009;27:4103–8.
23. Bender B, Jin J, Friberg L. A mechanism-based model of tumor quiescence and resistance in her2-negative metastatic breast cancer in patients receiving docetaxel or paclitaxel; 2017. p. 26. Abstract nr 7344.
24. Bender B. Pharmacometric models for antibody drug conjugates and taxanes in HER2+ and HER2- breast cancer. Uppsala: Uppsala University; 2016.
25. Petersson KJF, Hanze E, Savic RM, Karlsson MO. Semiparametric distributions with estimated shape parameters. Pharm Res 2009;26:2174–85.
26. Nguyen THT, Mouksassi M-S, Holford N, Al-Huniti N, Freedman I, Hooker AC, et al. Model evaluation of continuous data pharmacometric models: metrics and graphics. CPT Pharmacomet Syst Pharmacol 2017;6:87–109.
27. Plan EL. Modeling and simulation of count data. CPT Pharmacomet Syst Pharmacol 2014;3:e129.
28. Sheiner LB, Stanski DR, Vozeh S, Miller RD, Ham J. Simultaneous modeling of pharmacokinetics and pharmacodynamics: application to d-tubocurarine. Clin Pharmacol Ther 1979;25:358–71.
29. Jacqmin P, Snoeck E, van Schaick EA, Gieschke R, Pillai P, Steimer J-L, et al. Modelling response time profiles in the absence of drug concentrations: definition and performance evaluation of the K-PD model. J Pharmacokinet Pharmacodyn 2007;34:57–85.
30. Beal S, Sheiner L, Boeckmann A, Bauer R, editors. NONMEM 7.4 users guides (1989–2018). Gaithersburg, MD: ICON plc.
31. Schindler E, Amantea MA, Karlsson MO, Friberg LE. A pharmacometric framework for axitinib exposure, efficacy, and safety in metastatic renal cell carcinoma patients. CPT Pharmacomet Syst Pharmacol 2017;6:373–82.
32. Claret L, Gupta M, Han K, Joshi A, Sarapa N, He J, et al. Evaluation of tumor-size response metrics to predict overall survival in Western and Chinese patients with first-line metastatic colorectal cancer. J Clin Oncol 2013;31:2110–4.
33. Claret L, Jin JY, Ferté C, Winter H, Girish S, Stroh M, et al. A model of overall survival predicts treatment outcomes with atezolizumab versus chemotherapy in non-small cell lung cancer based on early tumor kinetics. Clin Cancer Res 2018; 24:3292–8.
34. Zheng Y, Narwal R, Jin C, Baverel PG, Jin X, Gupta A, et al. Population modeling of tumor kinetics and overall survival to identify prognostic and predictive biomarkers of efficacy for durvalumab in patients with urothelial carcinoma. Clin Pharmacol Ther 2018;103:643–52.
35. Tardivon C, Desmée S, Kerioui M, Bruno R, Wu B, Mentré F, et al. Association between tumor size kinetics and survival in urothelial carcinoma patients treated with atezolizumab: implication for patient's follow-up. Clin Pharmacol Ther 2019;106:810–20.
36. Cohen SJ, Punt CJA, Iannotti N, Saidman BH, Sabbath KD, Gabrail NY, et al. Relationship of circulating tumor cells to tumor response, progression-free survival, and overall survival in patients with metastatic colorectal cancer. J Clin Oncol 2008;26:3213–21.
37. Cohen SJ, Punt CJA, Iannotti N, Saidman BH, Sabbath KD, Gabrail NY, et al. Prognostic significance of circulating tumor cells in patients with metastatic colorectal cancer. Ann Oncol 2009;20:1223–9.
38. Aggarwal C, Meropol NJ, Punt CJ, Iannotti N, Saidman BH, Sabbath KD, et al. Relationship among circulating tumor cells, CEA and overall survival in patients with metastatic colorectal cancer. Ann Oncol 2013;24:420–8.
39. Bidard F-C, Peeters DJ, Fehm T, Nolé F, Gisbert-Criado R, Mavroudis D, et al. Clinical validity of circulating tumour cells in patients with metastatic breast cancer: a pooled analysis of individual patient data. Lancet Oncol 2014;15: 406–14.
40. de Bono JS, Scher HI, Montgomery RB, Parker C, Miller MC, Tissing H, et al. Circulating tumor cells predict survival benefit from treatment in metastatic castration-resistant prostate cancer. Clin Cancer Res 2008;14:6302–9.
41. Hou J-M, Krebs MG, Lancashire L, Sloane R, Backen A, Swain RK, et al. Clinical significance and molecular characteristics of circulating tumor cells and circulating tumor microemboli in patients with small-cell lung cancer. J Clin Oncol 2012;30:525–32.
42. Ferlay J, Colombet M, Soerjomataram I, Mathers C, Parkin DM, Piñeros M, et al. Estimating the global cancer incidence and mortality in 2018: GLOBOCAN sources and methods. Int J Cancer 2019;144:1941–53.
43. Rodrigues D, Longatto-Filho A, Martins SF. Predictive Biomarkers in colorectal cancer: from the single therapeutic target to a plethora of options. BioMed Res Int 2016;2016:6896024.
44. Chun YS, Vauthey J-N, Boonsirikamchai P, Maru DM, Kopetz S, Palavecino M, et al. Association of computed tomography morphologic criteria with pathologic response and survival in patients treated with bevacizumab for colorectal liver metastases. JAMA 2009;302:2338–44.
45. Van Cutsem E, Cervantes A, Adam R, Sobrero A, Van Krieken JH, Aderka D, et al. ESMO consensus guidelines for the management of patients with metastatic colorectal cancer. Ann Oncol 2016;27:1386–422.
46. Cabel L, Proudhon C, Gortais H, Loirat D, Coussy F, Pierga J-Y, et al. Circulating tumor cells: clinical validity and utility. Int J Clin Oncol 2017;22:421–30.
47. Cristiano S, Leal A, Phallen J, Fiksel J, Adleff V, Bruhm DC, et al. Genome-wide cell-free DNA fragmentation in patients with cancer. Nature 2019;570:385–9.
48. Alix-Panabières C, Pantel K. Clinical applications of circulating tumor cells and circulating tumor DNA as liquid biopsy. Cancer Discov 2016;6:479–91.
49. Calabuig-Fariñas S, Jantus-Lewintre E, Herreros-Pomares A, Camps C. Circulating tumor cells versus circulating tumor DNA in lung cancer-which one will win? Transl Lung Cancer Res 2016;5:466–82.
50. Nanou A, Zeune LL, Wit S de, Miller CM, Punt CJ, Groen HJ, et al. Abstract 4464: Tumor-derived extracellular vesicles in blood of metastatic breast, colorectal, prostate, and non-small cell lung cancer patients associate with worse survival. Cancer Res 2019;79:4464.

AACR American Association for Cancer Research

Clinical Cancer Research

Comparing Circulating Tumor Cell Counts with Dynamic Tumor Size Changes as Predictor of Overall Survival: A Quantitative Modeling Framework

Ida Netterberg, Mats O. Karlsson, Leon W.M.M. Terstappen, et al.

Clin Cancer Res 2020;26:4892-4900. Published OnlineFirst June 11, 2020.